HEFAT2011
8th International Conference on Heat Transfer, Fluid Mechanics and Thermodynamics
11 July – 13 July 2011
Pointe Aux Piments, Mauritius

Effect of Mesh Grids on the Turbulent Mixing Layer of an Axisymmetric Jet

Rajagopalan S. Antonia, R.A. and Djenidi L.*
*Author for correspondence
School of Engineering,
University of Newcastle,
2308, NSW
Australia,
E-mail: lyazid.djenidi@newcastle.edu.au

ABSTRACT

This paper focuses on the effect that two different mesh grids have on the structure of the mixing layer of an axisymmetric jet. Detailed measurements of mean velocity and turbulent velocity fluctuations are made with an *X* hot-wire probe in the range $0.5 \leq x/d \leq 10$, where x is the longitudinal distance from the nozzle exit plane and d is the nozzle diameter. The grids are introduced just downstream of the nozzle exit plane: one completely covers the nozzle (full mesh or FM), the other covers the central, high speed zone (disk mesh or DM). With reference to the undisturbed jet, FM yields a significant reduction in the turbulence intensity and width of the shear layer whereas DM enhances the turbulence intensity and increases the width of the shear layer. Both grids suppress the formation of the Kelvin-Helmholtz instability in the mixing layer. Results are presented, mainly at $x/d = 5$, both in the spectral domain and in physical space. In the latter context, second and third-order structure functions associated with u (the longitudinal velocity fluctuation) and v (the lateral or radial velocity fluctuation) are presented. All mesh geometries have a more significant effect on the second-order structure function of u than on that of v. The third-order energy transfer term is affected in such a way that, relative to the undisturbed jet, its peak location is shifted to a smaller scale with FM is used and to a larger scale with DM. This is consistent with our observations that FM reduces the turbulence in the shear layer whilst DM enhances it. It is suggested that the large scale vortices that are formed at the edge of the grids play a significant role in the transfer of energy.

INTRODUCTION

Flow control in general and turbulence management and control in particular have received much attention over the past few decades. This is not surprising because of the potential industrial and economic benefits that can accrue. In the specific context of a jet, a flow of major industrial importance, turbulence enhancement can be beneficial in terms of mixing and the improved design of combustion chambers. Turbulence suppression can, on the other hand, result in a reduction in jet noise. A major outcome of turbulence research has been the identification of organized, vortical or coherent structures which play an important role in the flow development. The main thrust in flow control research seems to be the manipulation of and interference with these coherent structures whose presence in different turbulent flows has been well documented and their properties well established. For example, in a jet the initial mixing layer region is characterised by the existence of organised, periodic vortical structures that stem from a Kelvin-Helmholtz instability. The suppression of these structures can lead to a reduction in turbulence intensity whereas their enhancement can increase the turbulence and the mixing characteristics of the flow. The target of several flow control studies has been to formulate strategies for interfering with these structures in order to achieve the desired goal. Turbulence control schemes generally fall under two categories, namely active or passive. With active control, a small fluctuating energy at a suitable frequency and amplitude is added to the mean flow; the frequency at which the flow is excited can yield either a reduction or an enhancement of the turbulence. The frequency of the imposed excitation is generally either equal to a harmonic or a sub harmonic of the frequency of occurrence of the coherent structures in the unperturbed flow. In a jet, a periodic excitation can be imposed by using an acoustic speaker or a vibrating element either in the settling chamber or at the nozzle exit plane. One of the passive methods of flow control involves the use of slender bluff bodies (e.g. thin ring or cylinder) as flow control units that are placed at suitable locations in the jet (1, 5, 7-17). The interaction between the main flow and the wake generated by the slender object seems to provide an appropriate control for the flow development. There are other passive techniques such as the use of boundary layer tripping and nozzle exit shape modification. A hybrid technique that combines active and passive techniques has also been successfully employed in a jet by Parker et al (13). Such an approach may provide a more effective flow control compared to what can be achieved with either a passive technique or an active technique on its own.

The literature on flow control is quite extensive especially for plane and circular jets; see (2, 3, 4 and 8, 19) for reviews on several aspects of flow control. The formation of coherent structures, which are targeted in most if not all of the flow control strategies, and the identification of their properties have also been extensively looked at (3). The coherent vortical structures play a crucial role in the transport of mass, momentum and heat and hence any control that is exerted on these structures to modify their properties will significantly alter the turbulent stresses, transport and the growth rate. Some of the other developments in flow control strategy are based on the use of synthetic jets and spiral (swirl) jets. In this paper we present some of the significant results of jet turbulence control investigations based on measurements in an axisymmetric jet. The focus is mainly on the development of a passive control technique that involves the use of grids (meshes) of different geometry for both turbulence reduction and enhancement.

Nomenclature

d	[m]	Nozzle diameter
f_0	[Hz]	Kelvin-Helmholtz instability frequency
r	[m]	Separation along x between two points (structure functions)
Re_d	[-]	Reynolds number ($U_j d/\nu$)
St_d	[-]	Strouhal number ($f_0 d/U_j$)
U	[m/s]	Mean velocity
Uj	[m/s]	Jet exit velocity
U_∞	[m/s]	Free stream velocity
u	[m/s]	Longitudinal velocity fluctuation
v	[m/s]	Radial velocity fluctuation
u'	[m/s]	Rms of u
v'	[m/s]	Rms of v
x	[m]	Longitudinal distance from the nozzle lip
x_0	[m]	Virtual origin
y	[m]	Distance along radial direction with origin at the nozzle lip
$y_{0.1}$	[m]	Value of y where $U/U_j = 0.1$
$y_{0.5}$	[m]	Value of y where $U/U_j = 0.5$
$y_{0.9}$	[m]	Value of y where $U/U_j = 0.9$
δ	[m]	Boundary layer thickness at nozzle exit
$\delta*$	[m]	Boundary layer displacement thickness
θ_o	[m]	Boundary layer momentum thickness

EXPERIMENTAL CONDITIONS

Measurements are made in a low speed axisymmetric jet with a nozzle diameter of 54.4 mm. Air is supplied by a variable speed centrifugal blower to a diffuser, settling chamber followed by a 9 to1 contraction to the nozzle exit. The nozzle centre-line exit velocity U_j is maintained at a nominal value of 10 m/s which yields a Reynolds number Re, based on U_j and the nozzle diameter, of about 36100. A sketch (not to scale) of the nozzle, the location of the grids and the coordinate system employed are shown in Figure 1.

The mean velocity (U) and the longitudinal (u) and normal (v) velocity fluctuations are measured with a X-hot wire probe with 2.5 μm (Pt-Rh) sensing elements operated in constant temperature mode. The anemometer output is digitized using a 12 bit A to D converter at 10 kHz per channel and the data are stored on a PC for further processing.

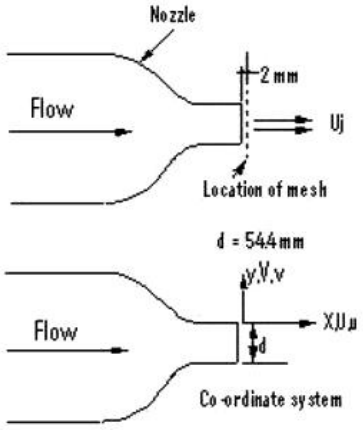

Figure 1. Sketch of nozzle and locations of mesh grids.

Measurements in the flow unperturbed by the grids, here identified as the free jet (FJ), provide the base data for comparison with the perturbed flows. The two grids (Figure 2) are

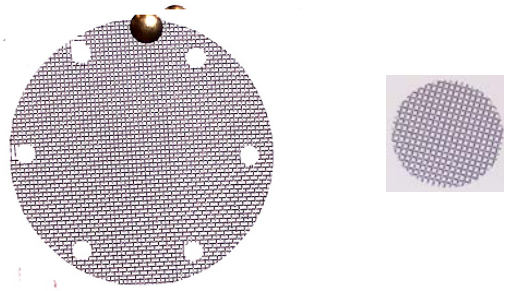

Full Mesh **Disk Mesh**

Figure 2. Grid mesh geometries.

(i) a disk-like mesh (DM) with an outer diameter of 30 mm so that it covers most of the potential core and (ii) the full mesh (FM) that covers the entire nozzle cross section. The grids are made of 0.5 mm diameter wire with a 1.25 mm square aperture, yielding a solidity of 0.64. For the FM flow, the mesh is placed outside the nozzle at a distance of 2mm downstream of the exit plane. Care is taken to align DM concentrically with the nozzle and the meshes are monitored through a telescope to ensure that they do not vibrate in the flow. Measurements are made at several downstream locations in the range $0 \le x/d \le 10$. For the free jet and the annular mesh flows, U_j is fixed at 10 m/s on the centre line at the nozzle exit plane; however, because of the presence of the grid, for the disk mesh and full mesh flows the velocity immediately downstream was unsteady and the value of U_j was set at 10 m/s at two diameters downstream. Stephens et al (16), Burattini et al (1) and Lehman et al (5) have also used a similar approach. The hot wire is mounted on an

electronic traversing system for longitudinal (x) movement and the normal (y) movement was achieved by using a height gauge with a least count of 0.01 mm. The nozzle exit boundary layer mean velocity profile is measured with a single hot wire (diameter=2.5 μm) probe.

RESULTS AND DISCUSSION

Initial conditions

The nozzle exit boundary layer state, viz. laminar, transitional or turbulent, influences the mixing layer development. A thin laminar boundary results in the occurrence of strong azimuthal or spanwise vortices which amalgamate to produce vortex pairing interactions. These vortices are also associated with an intense normal velocity fluctuation. A turbulent exit boundary layer produces a mixing layer where the vortical structures are either weak or do not exist. For the present study, the boundary layer at the nozzle exit is laminar – some work has also been done with a turbulent boundary layer, obtained by placing FM upstream of the nozzle – this will be reported elsewhere.

The boundary layer velocity profile was measured for the undisturbed jet; it was assumed that the boundary layer profiles when the grids are inserted will not be significantly different from that for the undisturbed jet. The boundary layer velocity profile is shown in Figure 3 together with the Blasius distribution. It can be seen that for the undisturbed jet, the boundary layer at the nozzle exit is pseudo-laminar with a shape factor H of 2.43 compared to a value of 2.6 for Blasius. The departure from Blasius is reasonable in view of the favourable pressure gradient in the contraction and can be reconciled with a Falkner-Skan solution corresponding to this pressure gradient. The turbulence intensity (u'/U_∞) at a location 0.3 mm away from the wall is is 1.2 % for the undisturbed jet.

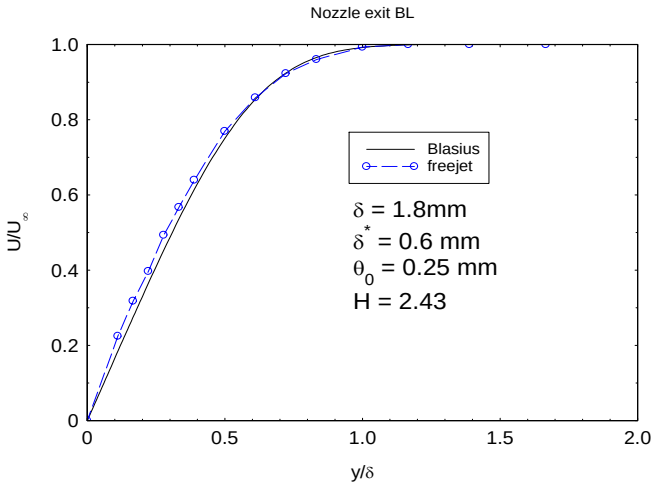

Figure 3 Boundary layer velocity profile at nozzle exit.

Mean velocity and rms intensities

Normalised mean velocity distributions at $0.5 \leq x/d \leq 5$ for the free jet are presented in Figure 4. Here the lateral coordinate (y) is normalised by (x-x_0) where x_0 is the virtual origin. The latter was inferred by plotting the streamwise loci of $y_{0.1}$, $y_{0.5}$ and $y_{0.9}$ (or values of y which correspond to U/Uj = 0.1, 0.5 and 0.9) respectively against x/d; all three loci yielded the same value of x_0 (approximately 10 mm). Figure 4 indicates that normalised mean velocity distributions exhibit good similarity for $x/d > 0.5$ which is characteristic of a mixing layer with a laminar exit boundary layer.

The mean velocity and rms velocity fluctuation (u' and v') distributions at x/d = 5 are shown in Figure 5 for the undisturbed jet as well as for FM and DM. Compared to the undisturbed jet, FM seems to exhibit an increased potential core region and a reduction in shear layer width. For DM, there is an excess velocity in the gap between the nozzle inner wall and the

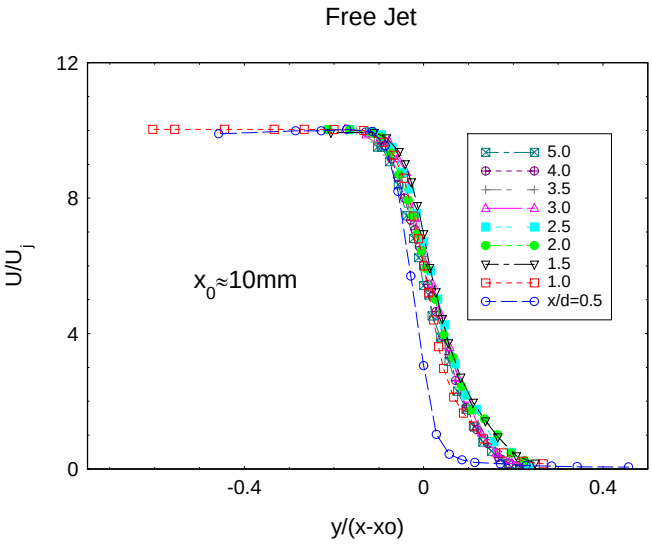

Figure 4 Mean velocity profiles at several streamwise locations in the mixing layer of the undisturbed jet.

outer edge of the mesh which is due to the fact that U_j was set to 10 m/s on the centreline, downstream of the disk mesh. As our aim was to maintain the same jet Reynolds number, this excess is unavoidable. Hence DM yields a large increase in shear layer width as well as mean velocity. The use of FM decreases both u' and v', the latter being more affected than the former. Such a reduction suggests that FM inhibits the formation of large structures resulting in a decrease in turbulence intensity and shear layer width and an increase in the longitudinal extent of the potential core. DM yields a large increase in turbulence intensity and a concomitant increase in the width of the shear layer. Similar results were obtained by Tong and Warhaft (17) for a circular jet perturbed by a ring and by Rajagopalan and Antonia (14, 15) for a plane jet perturbed by thin cylinder.

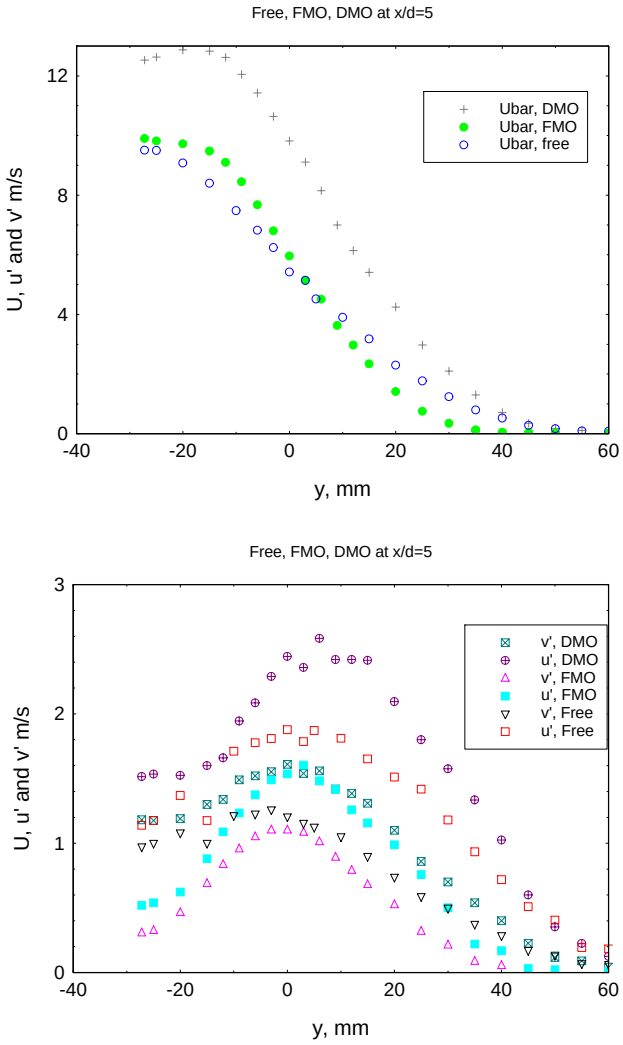

Figure 5 Mean Velocity (top) and rms (bottom) Turbulent Velocity Fluctuations

The important conclusions that can be drawn from Fig 5 are that

- FM increases the extent of the potential core and reduces growth rate of the mixing layer. For example at x/d = 5, the width of the FM jet, estimated from $y_{0.1}$ and $y_{0.9}$, decreased to 36 mm compared to 52 mm for the undisturbed (or 'free') jet.

- FM reduces the turbulence intensity by inhibiting the Kelvin-Helmholtz instability. Spectral data (not shown here) yielded a Kelvin-Helmholtz instability frequency of 533 Hz whereas no discernible peak could be observed for the FM flow. However, for the DM jet, a broad spectral peak was observed at a reduced frequency which may be associated with the structures formed at the mesh edge, similar to that observed by Oguchi and Inoue (6) and Zhou and Antonia (20).

- DM leads to a larger growth rate of the mixing layer and increases the turbulence intensity appreciably. At x/d=5, u' for the DM jet had a maximum value of 2.6 m/s compared to the values of 1.6 and 1.9 m/s for the FM and free jet flows respectively.

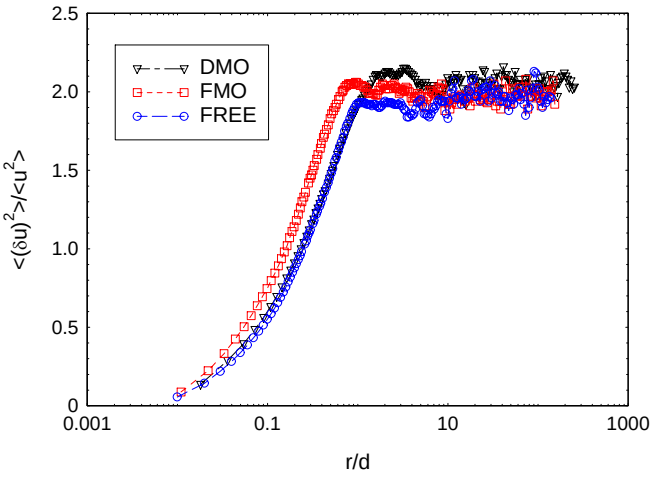

Figure 6 Second-order structure functions of u at x/d = 5 (y = 0)

The turbulence suppression that is obtained with FM is similar to that obtained by introducing a slender cylinder or a ring as observed by several investigators.

Structure functions

We consider next the behaviour of the second-order moments of the velocity incremements $\delta u = u(x+r)-u(x)$ and $\delta v = v(x+r)-v(x)$, where the separation r is inferred from the temporal increments $u(t)-u(t+\tau)$ and $v(t)-v(t+\tau)$ by assuming Taylor's hypothesis. The turbulent energy structure function $<(\delta q)^2> = <(\delta u)^2> + <(\delta v)^2> + <(\delta w)^2>$ is formed by assuming axisymmetry, viz.

$$<(\delta v)^2> = <(\delta w)^2> \qquad (1)$$

so that

$$<(\delta q)^2> = <(\delta u)^2> + 2<(\delta v)^2> \qquad (2).$$

The transport equation for $<(\delta q)^2>$, which can be interpreted as a scale-by-scale budget for the turbulent energy at any given location in the flow. A simplified form of this equation can be written as

$$-\frac{\left\langle \delta u (\delta q)^2 \right\rangle}{\langle \varepsilon \rangle r} + \frac{2\nu}{\langle \varepsilon \rangle r}\frac{d}{dr}\left\langle (\delta q)^2 \right\rangle + \frac{I_q}{\langle \varepsilon \rangle r} = \frac{4}{3}$$

where $<\varepsilon>$ is the mean energy dissipation rate and I_q represents the inhomogeneity in the flow. The above equation is strictly valid for locally homogeneous isotropic turbulence. For the

present purpose, we have formed the third-order term $<\delta u(\delta q)^2>$ by assuming that axisymmetry is also valid, viz, $<\delta u(\delta q)^2> \approx <(\delta u)^3> + 2<\delta u(\delta v)^2>$. We have not yet investigated I_q. For decaying grid turbulence $I_q = -\frac{U}{r^2}\int_0^r s^2 \frac{\partial}{\partial x}\left\langle (\delta q)^2 \right\rangle ds$, i.e. its contribution comes entirely from the streamwise decay of $<(\delta q)^2>$. In the present flow, we expect that near $y = 0$, I_q should mainly reflect the contributions from the major terms in the one-point energy budget, i.e. the production and diffusion of $< q^2 >$, as inferred from example from the energy budget measured by Wygnanski and Fiedler [18].

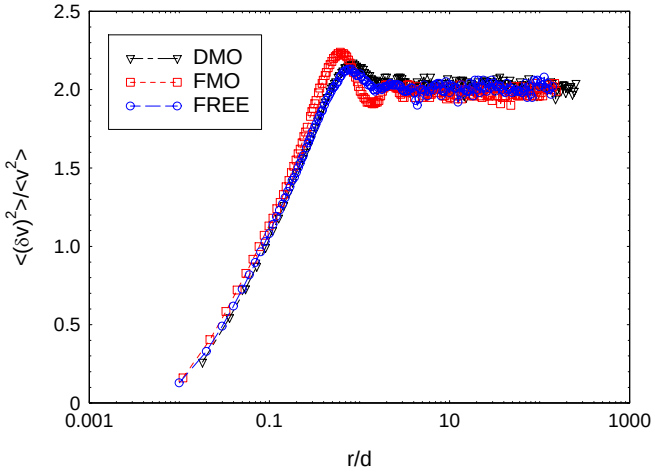

Figure 7 Second-order structure functions of v at $x/d = 5$ ($y = 0$)

Distributions at $y = 0$ (x/d=5) of $<(\delta u)^2>$ and $<(\delta v)^2>$, normalized by the variances of u and v, are plotted in Figures 7 and 8 vs r/d. At large enough r/d, typically about 10, they reach the expected value of 2. The effect of the grids is larger on $<(\delta u)^2>$ $/<u^2>$ than for $<(\delta v)^2>$ $/<v^2>$ or indeed $< (\delta q)^2 > / < q^2 >$ (Fig 9). In the latter figure, $< q^2 >$ is assumed to be given by $< u^2 > +2 < v^2 >$; when r/d is about 1, $< (\delta q)^2 > / < q^2 >$ reaches its limit of 2. In particular, distinct peaks appear in Fig 7 for FM and DM. In figures 7, 8 and 9, the peak for FM is at a smaller r/d than the peak for DM.

Distributions of $<\delta u(\delta\alpha)^2>$ (α stands for u, v or q) are shown in Figures 10, 11 and 12 for each of the three cases. Note that the magnitude of $<\delta u(\delta v)^2>$ is smaller than $<(\delta u)^3>$ and changes sign beyond the value of r/d at which $<(\delta u)^3>$ and $<\delta u(\delta v)^2>$ first peak. The distributions of $<\delta u(\delta q)^2>$,normalized by u'^3, are plotted in Fig 13. It is noticeable that for FM the peak of $<\delta u(\delta q)^2>$ is at a smaller r/d than that of the undisturbed jet. On the other hand, the peak for DM is at a larger r/d that that for the undisturbed jet. The maximum transfer of energy thus occurs at smaller and larger scales, respectively for FM and DM, by comparison to the undisturbed jet. This seems to be consistent with the reduction in turbulence intensity for FM and its enhancement for DM.

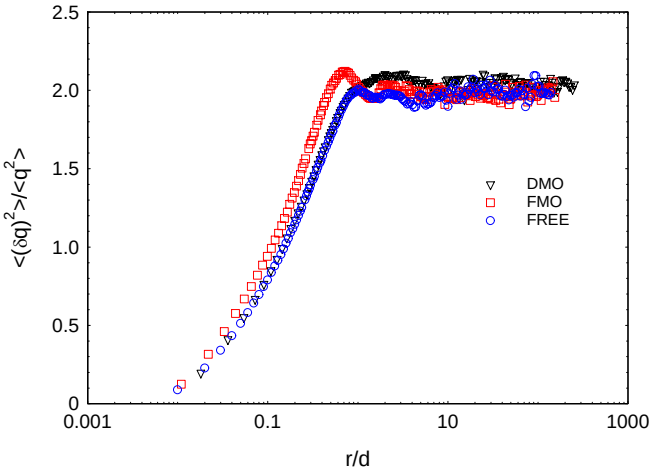

Figure 8 Energy structure function, as defined by Eq (2), at $x/d = 5$ ($y = 0$)

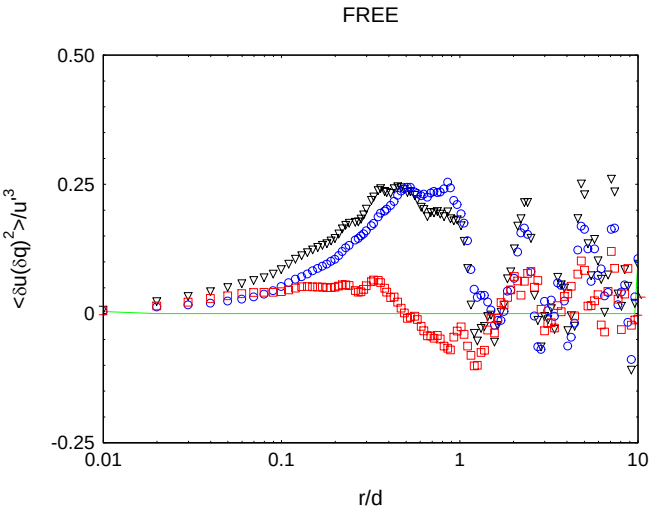

Figure 9 Third-order energy transfer term $<\delta u(\delta q)^2>$ (black symbols) and its components $<(\delta u)^3>$ (blue symbols) and $<\delta u(\delta v)^2>$(red symbols) for the undisturbed jet. ($x/d = 5$, y=0)

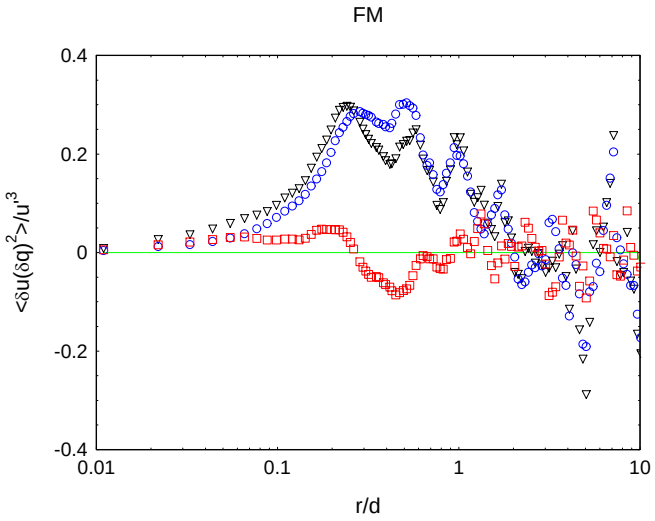

Figure 10 Third-order energy transfer term $<\delta u(\delta q)^2>$ (black symbols) and its components $<(\delta u)^3>$ (blue symbols) and $<\delta u(\delta v)^2>$(red symbols) for FM. ($x/d = 5, y = 0$)

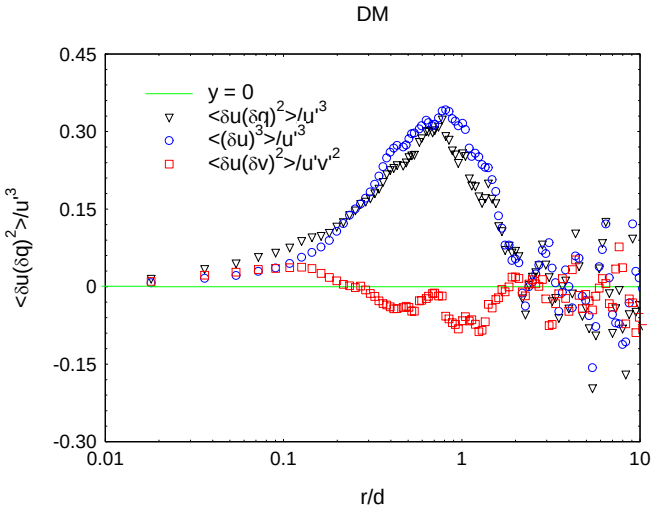

Figure 11 Third-order energy transfer term $<\delta u(\delta q)^2>$ (black symbols) and its components $<(\delta u)^3>$ (blue symbols) and $<\delta u(\delta v)^2>$(red symbols) for DM. ($x/d = 5, y = 0$)

Conclusions

The present study establishes that the turbulence intensity and growth rate of a mixing layer can be either enhanced or reduced by using mesh grids that cover the jet nozzle either partially (DM) or completely (FM). Turbulence reduction is achieved by inhibiting the formation of organized, vortical structures through the suppression of the Kelvin-Helmholtz instability

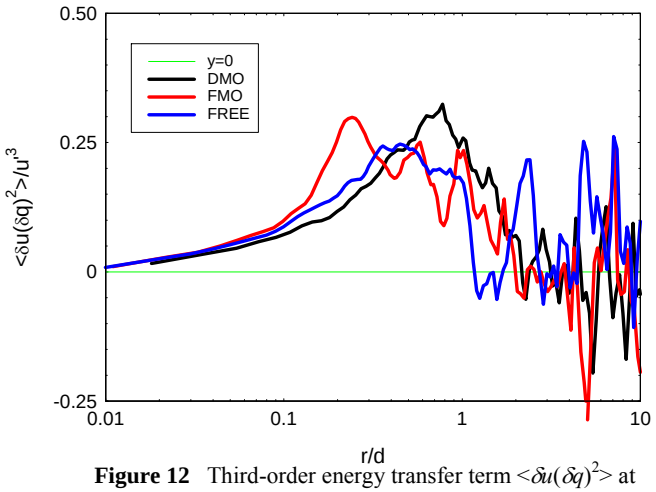

Figure 12 Third-order energy transfer term $<\delta u(\delta q)^2>$ at $x/d = 5$ ($y = 0$). Blue:undisturbed jet, Red: FM, Black: DM.

The present results, in particular those related to the third-order energy structure functions, demonstrate that an enhancement in turbulence intensity and growth rate can be achieved by using a disk mesh grid (DM). The large structures that are formed at the edge of the mesh excite the shear layer (or inject energy) in such a way that the maximum energy transfer rate now occurs at a larger scale than in the undisturbed mixing layer. By contrast, the effect of the full mesh grid (FM) is to shift the maximum energy transfer rate to a smaller length scale than for the undisturbed mixing layer, resulting in a decrease in trurbulence intensity and growth rate.

ACKNOWLEDGMENTS

The authors acknowledge the financial support of the Australian Research Council and Ken Sayce for his expert technical assistance.

REFERENCES

[1] Burattini P., Antonia R.A., Rajagopalan S. and Stephens M., 2004, Effect of Initial Conditions on the Near Field Development of a Round Jet. *Expts. Fluids,* **37,** 56-64

[2] Gutmark E.J. and Grinstein F.F., 1999, Flow Control with Noncircular Jets. In Lumley JL, Van Dyke M, Reed H ed. *Annual review of Fluid Mechanics*, **31**, 239-272

[3] Husain H.S., Bridges J.E. and Hussain F., 1988, Turbulence Management in Free Shear Flows by Control of Coherent Structures. In Hirata M, Kasagi N ed. *Transport Phenomena in Turbulent Flows,* Hemisphere Publication, 111-130

[4] Hussain A.K.M.F., 1983, Coherent Structures – Reality or Myth. *Phys. Fluids*, **26**(10), 2816-1850

[5] Lehman R., Rajagopalan S., Burattini P., Antonia R.A., 2004, Axisymmetric Jet Control Using Passive Grids. Behnia M, Lin W, McBain GD ed. *Proc. 15 Australasian Fluid Mechanics Conference,* Sydney

[6] Oguchi H. and Inoue, O., 1984,Mixing Layer Produced by a Screen and its Dependence on Initial Conditions., *J.Fluid Mech.,***142**, 217-231

[7] Olsen J.F., Jet Turbulence Control. 2001, *Ph.D. Thesis*, University of Newcastle, Australia

[8] Olsen J., Rajagopalan S. and Antonia R.A., 1999, Control of Jet Turbulence. In Pandalai GAV ed. *Recent Research Developments in Fluid Dynamics,* 87-119

[9] Olsen J.F., Rajagopalan S. and Antonia R.A., 2003 a, Preferred Modes and Jet Column Modes in a Plane Jet and in a Passively Modified Plane Jet, Hanjalic K, Nagano Y, Tummers M ed. *Turbulence, Heat and Mass Transfer 4*, Begell House Inc

[10] Olsen J.F., Rajagopalan S. and Antonia R.A., 2003 b, Jet Column Modes in Both a Plane Jet and a Passively Modified Plane jet Subject to Acoustic Excitation. *Expts. Fluids,* **35**, 278-287

[11] Parker R., Rajagopalan S. and Antonia R.A., 2001, Control of an Axisymmetric Jet Using a Passive Ring. Dally BB ed. *Proc. 14 Australasian Fluid Mechanics Conference*, Adelaide, Australia

[12] Parker R., Rajagopalan S. and Antonia R.A., 2003a, Control of an Axisymmetric Jet Using a Passive Ring. *Exp.Thermal and Fluid Sci.,* **27**, 545-552

[13] Parker R., Rajagopalan S. and Antonia R.A., 2003b, Interaction of Acoustic Excitation with a Passive Ring in an Axisymmetric Jet. Kasagi N et al ed. *Turbulence and Shear Flow Phenomena 3,* Japan

[14] Rajagopalan S. and Antonia R.A., 1997, Turbulence Modification Using a Thin Cylinder in the Mixing Layer of a Plane Jet. Tulapurkara EG, Gowda BHL ed. *Proc. Seventh Asian Congress of Fluid Mechanics,* Chennai, India

[15] Rajagopalan S. and Antonia R.A., 1998, Turbulence Reduction in the Mixing Layer of a Plane Jet Using Small Cylinders. *Expts. Fluids,* **25,** 96-103

[16] Stephens M., Rajagopalan S., Burattini P., Antonia R.A., 2004, Axisymmetric Shear Flow Behind a Honeycomb. Wijetunge JJ ed. *Proc. Tenth Asian Congress of Fluid Mechanics,* Sri Lanka

[17] Tong C. and Warhaft Z., 1994, Turbulence Suppression in a Ring by means of a Fine Ring. *Phys. Fluids*, **6**(1), 328-333

[18] Wygnanski I. and Fiedler, H.E. 1970, The two-dimensional mixing region, *J. Fluid Mech.* **41**, 327-361.

[19] Zaman K.B.M.Q. and Hussain A.K.M.F., 1981, Turbulence Suppression in Free Shear Flows by Controlled Excitation. *J. Fluid Mech.,* **103**, 133-159

[20] Zhou Y. and Antonia R.A., 1995, Memory Effects in a Plane Turbulent Wake. *Expts. Fluids*, **19**, 112-120